Effect of electrostatic interaction on the retention and remobilization of colloidal particles in porous media

Kottsova, Anna K.; Mirzaie Yegane, Mohsen; Tchistiakov, Alexei A.; Zitha, Pacelli L.J.

DOI
10.1016/j.colsurfa.2021.126371

Publication date
2021

Document Version
Final published version

Published in
Colloids and Surfaces A: Physicochemical and Engineering Aspects

Colloids and Surfaces A: Physicochemical and Engineering Aspects 617 (2021) 126371

Contents lists available at ScienceDirect

Colloids and Surfaces A: Physicochemical and Engineering Aspects

journal homepage: www.elsevier.com/locate/colsurfa

Effect of electrostatic interaction on the retention and remobilization of colloidal particles in porous media

Anna K. Kottsova [a,*], Mohsen Mirzaie Yegane [b], Alexei A. Tchistiakov [a], Pacelli L.J. Zitha [b]

[a] Skoltech Center for Hydrocarbon Recovery, Skolkovo Institute of Science and Technology, Bolshoy Boulevard 30, bld. 1, Moscow, 121205, Russia
[b] Department of Geoscience and Engineering, Delft University of Technology, Stevinweg 1, Delft, 2628 CN, the Netherlands

GRAPHICAL ABSTRACT

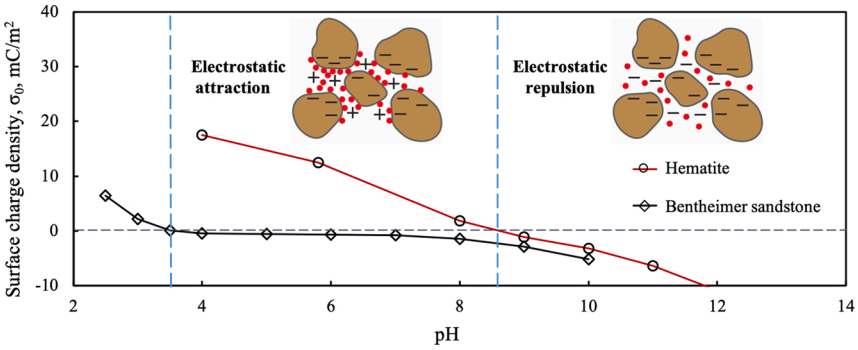

ARTICLE INFO

Keywords:
Fines
Hematite particles
Point of zero charge
van der Waals
Electrostatic
Interactions

ABSTRACT

We investigate the effect of pH on external hematite colloidal particles entrapment and remobilization by core-flood experiments combined with X ray computed tomography. Suspensions of calibrated hematite colloidal particles were injected into Bentheimer sandstones sample, composed mainly of well-sorted quartz and small clay fraction (up to 1 wt%), consisting mainly of kaolinite. We have found that permeability impairment due to an external cake build-up can be reversed when pH exceeds the point of zero charge of hematite particles. This effect could be successfully interpreted by the switching of the surface charge of hematite particles from positive to the negative, similar to the rock surface. The experimentally verified pH-controlled electrostatic retention and remobilization technique can be extended to other colloidal particles, having pH-dependent surface charge, including natural clay minerals in hydrocarbon and geothermal reservoirs. Therefore, varying pH of injected fluid can be applied for targeted external cake build-up and transportation of colloidal particles within a reservoir.

1. Introduction

Colloidal fines migration is a common phenomenon in various industrial processes relying on fluid flow in porous media, including hydrology [1,2], geothermal engineering [3,63,72], gas production from hydrate-bearing sediments [4], well-bore drilling [5,62,73]; and

* Corresponding author.
E-mail address: Anna.Kottsova@skoltech.ru (A.K. Kottsova).

https://doi.org/10.1016/j.colsurfa.2021.126371
Received 22 November 2020; Received in revised form 8 February 2021; Accepted 20 February 2021
Available online 24 February 2021

enhanced oil recovery (EOR), where low salinity water injection emerged as a new approach to mobilize additional oil [6–9]. Water injection applied within these processes can cause impairment of permeability due to blockage of pores at the borehole walls by particles, suspended in the water, or due to entrapment of migrating in-situ clay particles in pore throats within the reservoir.

Fines migration in porous media has been intensively investigated in the last few decades [10,25,74–78]. It was established that attachment or detachment of colloidal particles from pore walls and following up their migration in porous media are determined by the balance of forces acting between the particles and the rock mineral grains surfaces. The attachment occurs thanks to London – van der Waals attraction forces. The detachment can be triggered by combined effect of repulsive forces such as the electrostatic repulsion of overlapping electrical double layers (EDL), if the surface charge of clay particles and the rock matrix has the same sign, structural forces of bound water, hydrodynamic drive of flowing fluid. [1–17,61].

The electrostatic repulsion considerably depends on the fluid salinity as the latter changes ζ-potentials of the interacting surfaces. The repulsion between a clay particle and a pore wall decreases with the rise of ionic strength of the pore aqueous solution and increases when the fluid salinity drops. It was experimentally demonstrated, that at low salinity of the injected fluid in-situ particles could be detached from the rock matrix surface and deposited downstream that led to significant reduction of the rock permeability [3,6,11,14–16,18–21,79].

Besides salinity, the electrostatic interaction between clay particles and the rock mineral matrix is controlled by the pore fluid pH [11,18,19,22–26]. It was experimentally confirmed that an increase of pH above a certain critical value causes charge reversal of natural clay ζ-potential from positive to negative. The critical pH value, when ζ-potential becomes zero, is called point of zero charge [27–29]. For clay particles, the point of zero charge (PZC) can vary significantly depending on their mineralogy and crystal structure, however at pH values feasible for sandstone formations it is always larger than the point of zero charge of quartz that is commonly a predominant component of the sandstones matrix [28,30–33]. This means that at certain pH values, in-situ clay particles as well as external colloidal particles, present in the fluid injected in the formation, can have a surface charge of the same or opposite sign with the charge of the rock pore surface. This means that we can theoretically manage migration and retention of in-situ and external colloidal particles within a reservoir porous medium by varying pH. Some research on this subject has already been done. For example Kumar et al. [26] has experimentally shown that an increase of pH causes increase of the magnitude of the long-range repulsion between a SiO2 tip and a silica facet of kaolinite. The experiments were done within the range of pH above kaolinite's PZL and thus no charge reversal occurred. Kobayashi et al. [24] have investigated the effect of pH alteration on retention of latex particles by a zirconia bed and concluded that pH increase had minor effect on the retention in comparison with salinity rise.

Although considerable efforts have been made to investigate the effect of pH variation on external particle migration and retention by different materials today we still do not have confident and experimentally confirmed methodology of these process management in natural reservoirs.

The main objective of this research was to examine the possibility of artificial management of external colloidal particles retention by natural sandstone matrix and remobilization by gradual increase of pH of the injected fluid above the mineral point of zero charge. In previous studies pressure and effluent data were mainly used for monitoring fines migration within rock porous media, in the present study next to differential pressure measurements we applied X-ray tomography for tracking the migration of remobilized particles. Hematite particles were chosen as model particles because of their pH-dependent surface charge, distinguishable red color, and high density and X-ray attenuation capacity, which make them detectable for CT-assisted core-flood experiments. Bentheimer sandstone was used as the model porous medium. Prior to core-flood experiments, characterization of the rock and particles properties was performed and colloidal stability of the hematite suspension at various ionic strength and pH was studied by the DLVO theory. For core-flood experiments, a suspension of hematite particles was injected to deposit the particles within the porous media. Thereafter, deionized water with gradually increasing pH above the IEP of hematite particles was injected to give rise to a repulsion term between particles and sandstone surface and consequently to remobilize the deposited particles. We establish theoretical and experimental conclusions that presumably can be extended to other minerals with pH-dependent surface charge, including natural minerals in porous media.

The paper proceeds with description of materials and methods used for the experiments, where both preparation steps and experimental methodology are illustrated. Then, the experimental results are shown, followed by the general discussion and conclusions.

2. Materials and methods

2.1. Porous medium

The core-flood experiments were performed with Bentheimer sandstone of Early Cretaceous age from the south-western part of the Lower Saxony Basin. Bentheimer sandstone outcrop samples are often used as model natural porous medium for laboratory studies because of their lateral continuity and block scale homogeneous nature [34]. The high permeability and large pore size of Bentheimer samples make it an appealing candidate to study the migration of colloidal particles in porous media and the ensuing permeability reduction. Bentheimer sandstone, consists of more than 85 % of pore throats have a size larger than 10 μm and only 5% of them are smaller than 5 μm [34]. Table 1 shows the physical properties of Bentheimer core samples used to conduct the core-flood experiments. After cutting and drying the cores in an oven for up to 48 h at 60 ± 1 °C, the cores were placed in molds and encased in an epoxy resin to prevent bypassing the flow alongside the core. The penetration depth of the resin into the core was nearly 1.0 mm. Thereafter, the cores were precisely machined to an effective diameter of 3.8 ± 0.1 cm and a length of 17.0 ± 0.1 cm. The machined samples were dried for 15 h in an oven at 40 ± 1 °C. The porosities of the core samples were measured by the Helium gas expansion method. The permeability of the cores was estimated using Darcy's law, by flowing 5000 ppm NaCl brine at different rates within the core and recording the pressure drop. It should be noted that the characterization of the rock with XRD analysis and potentiometric titration measurements were performed on the rock sample pulverized to 1 μm powder.

2.2. Chemicals

Hematite (α-Fe_2O_3 with density equal to 5.24 g/cm^3) particles were supplied by Sigma-Aldrich in powder form with. The high density of the particles results in high attenuation of X-rays relative to quartz, the main component of the sandstone. The diameter of an individual particle was < 50 nm, as reported by the manufacturer, which was obtained from

Table 1
Properties of Bentheimer core samples.

Components	Quartz 99.3 ± 0.1 wt%	Kaolinite 0.7 ± 0.1 wt%
Porosity	24.4 ± 0.2 %	
Initial Permeability	Exp. 1 1770 ± 20 mD	Exp. 2 1400 ± 20 mD

Darcy (D) - permeability of the porous medium through which the flow of 1cm3 of fluid with viscosity of 1 cp in 1 s under the differential pressure of 1 atm, where the porous medium has cross-sectional area of 1 cm2 and length of 1 cm. 1 mD ≈ 1 μm^2·10^{-3}.

BET; however, they had a strong tendency to aggregate and form larger particles, therefore in this study we further refer to them as colloidal particles. Moreover, as mentioned, hematite particles had a distinguishable red color that simplified their detection in effluent and during the microscopic examination of the sample slab after core-flood experiments. Sodium chloride (NaCl) used for brine preparation was purchased from Sigma-Aldrich as well. The base (1 M NaOH) and acid (1 M HCl) used for pH adjustment, were supplied by Merck KGaA.

Aqueous suspensions of hematite were used to deposit particles inside the rock porous media. Earlier studies have shown that aggregation of hematite particles increases drastically with the addition of a small quantity of salt into the aqueous solution [35,36]. This is supported by our analysis of the colloidal stability of hematite suspensions. Therefore, in these experiments, we use hematite suspension in ultrapure deionized water (DI water). As for initial saturation of the core, 5000 ppm NaCl brine was used to prevent clogging of pores with released in-situ clay particles before the beginning of the experiment.

2.3. Preparation of hematite suspension

In order to avoid air entrapment inside of the hematite aggregates and produce an air-free stable suspension of hematite particles, the following preparation procedure was applied. First, the particles were placed into a vacuum, then saturated with CO_2 and after secondary vacuuming mixed with deionized water and stirred (Fig. 1). This was followed by sonication at the power of 550 W, 20 kHz, and an amplitude of 20 %. The applied procedure allowed preparing a colloidally stable suspension with no observable sedimentation. The pH of the prepared suspension was measured to be 5.8 ± 0.1. Hematite suspension of 250 ppm concentration prepared in deionized water was applied in flooding tests. During the core-flood experiments, the suspension in the tank was continuously stirred in order to maintain its homogeneity.

2.4. Characterization of rock and hematite particles

2.4.1. XRD analysis

XRD analysis was performed to determine the composition of the rock. The XRD data were obtained on a Bruker D8 Advance diffractometer equipped with a Bragg-Brentano geometry and Lynxeye position sensitive detector and using Cu Kα radiation. The pulverized rock was placed into an appropriate holder and its surface was made as flat as possible prior to the analysis. The scans were done with rotation on, at 45 kV and 40 mA. The measurement was performed with a coupled θ -2θ scan with a step size of 0.025° and time per step of 2 s. The Semi-quantitative (S-Q) approach was used to approximate the fractions of the identified phases. The fractions were calculated with Bruker Diffrac. Eva software using the height of the peaks after ka2 stripping and the ratio I/Icor from the ICDD PDF-4 + 2020 database.

2.4.2. Potentiometric mass titration

The potentiometric mass titration (PMT) method was used to identify the point of zero charge (PZC) of the rock. 100 mL of 1500 ppm NaCl (~ 0.025 mM) solution, as the background solution, was put into three different flasks. The pulverized rock with different masses of 2.5, 5.0, and 10.0 g was transferred to each flask. A blank solution without the addition of rock powder was also prepared. Before the experiment, the suspensions were stirred with a Teflon magnetic stirrer for 24 h to reach an equilibrium. Then potentiometric titrations were performed in a nitrogen atmosphere. First, 5 mL of 0.1 M NaOH was added to all flasks to deprotonate a significant portion of the surface sites, causing the surface to be negative. Next, each of these suspensions and the blank sample were titrated by addition of 0.1 M HCl to the cell in 10–15 steps. The samples were continuously stirred, except when the pH was recorded after every 2–5 min while the stirrer was switched off.

The pH-dependent surface charge density (σ_0) was determined based on the measured PMT data, according to the following equation [37]:

$$\sigma_0(pH) = \frac{F.(\Delta n_{sol,H^+}(pH) - \Delta n_0)}{mS_{BET}} \quad (1)$$

where F is the Faraday constant ($F = 96{,}500$ C/mol), m is the mass of the sample, S_{BET} is the rock specific surface area and Δn_0 is the pH-dependent amount of acid which is consumed on a sample with a very small mass (extrapolated to zero mass). The dissolution effect ($\Delta n_{sol,H^+}$) is obtained by comparison of the balance of protons ions in the potentiometric titration of suspensions with the blank potentiometric titration results according to the following equation:

$$\Delta n_{sol,H^+} = \Delta n_{acid(S)}(pH) - \Delta n_{acid(B)}(pH) \quad (2)$$

where $\Delta n_{acid(S)}(pH)$ and $\Delta n_{acid(B)}(pH)$ represent the balance of protons ions needed to be consumed to reach a certain pH for the suspension and blank respectively.

2.4.3. Zeta potential and particle size distribution

The zeta potential and hematite particles size distribution (PSD) in deionized water were measured using a Malvern Zetasizer Nano ZS at 25 ℃. Zeta potential is calculated by means of Henry's equation from the measured electrophoretic mobility. In order to enable measurements on this instrument the particles concentration was adjusted to provide a count rate of ca. 500 kcps. Samples were run in triplicate in the auto mode and the average was recorded. There was a pause of 30–60 sec between each run, for relaxation of the sample.

2.5. Hematite inter-particle interactions

Dispersed particles are subject to Brownian motion which causes frequent inter-particle collisions. The balance between inter-particle interactions determines whether the dispersion of hematite particles is colloidally stable. According to the DLVO theory [38–40], the total energy for the interaction between two unmodified spherical particles (V_t) with radius R, at separation distance h is given by the sum of van der Waals (V_v) and electrostatic (V_e) potentials:

$$V_t(x) = V_v(x) + V_e(x) \quad (3)$$

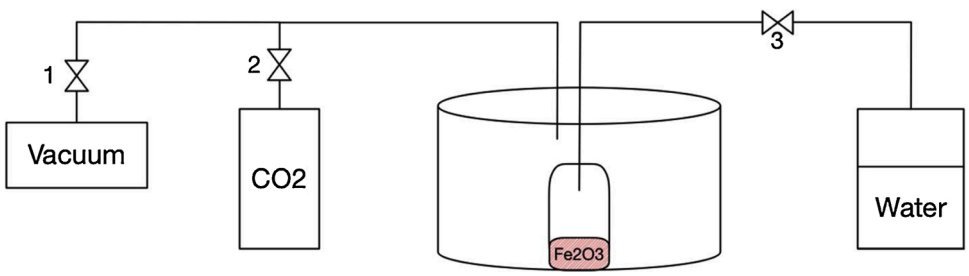

Fig. 1. Setup for preparation of hematite suspension. The hematite powder was vacuumed through valve 1 and CO_2 and water were further added through valves 2 and 3 respectively.

where x is the normalized separation distance equal to h/R. The van der Waals potential is [41]:

$$\frac{V_v(x)}{k_BT} = -\frac{\left(\sqrt{A_H} - \sqrt{A_W}\right)^2}{6k_BT}\left\{\frac{2}{x(x+4)} + \frac{2}{(x+2)^2} + \ln\left[\frac{x(x+4)}{(x+2)^2}\right]\right\} \quad (4)$$

where A_H and A_W are Hamaker constants for hematite particle and water, as the medium, respectively [42], k_B is the Boltzmann's constant and T is the absolute temperature. The electrostatic potential is described [43] by:

$$\frac{V_e(x)}{k_BT} = \frac{2\pi\varepsilon_0\varepsilon_r\psi_0^2 R}{k_BT}\ln[1 + \exp(-\kappa R x)] \quad (5)$$

where ε_0 is the vacuum permittivity, ε_r is the medium relative permittivity, ψ_0 is the surface potential and κ^{-1} is Debye length which is given by:

$$\kappa^{-1} = \left(\frac{\varepsilon_0\varepsilon_r k_BT}{2N_A e^2 I}\right)^{0.5} \quad (6)$$

where e is the electronic charge, N_A is the Avogadro's number, and I is the medium ionic strength [44]. Surface potential is estimated based on the zeta potential (ζ) using Eq. 7. The Equation is obtained by solving the Poisson − Boltzmann equation for a distribution of the point charges that decay as a function of the radial distance from the surface of charged particle [45]:

$$\psi_0 = \zeta\left(1 + \frac{1}{\kappa R}\right)\exp(1) \quad (7)$$

The pH-dependent surface charge density (σ_0) can be calculated according to Eqs. 8–9 [46]:

$$\sigma_0 = \frac{2\varepsilon_0\varepsilon_r\kappa k_BT}{e}\sinh\left(\frac{e\psi_0}{2k_BT}\right) \times \left[1 + \frac{1}{\kappa R}F(T) + \frac{1}{(\kappa R)^2}G(T)\right]^{1/2} \quad (8)$$

$$F(T) = \frac{2}{\cosh^2\left(\frac{e\psi_0}{4k_BT}\right)};\ G(T) = \frac{8ln\left[\cosh\left(\frac{e\psi_0}{4k_BT}\right)\right]}{\left(\frac{e\psi_0}{2k_BT}\right)} \quad (9)$$

Dispersions of particles stay kinetically stable if the potential barrier (V_{max}) is larger than $\sim 16/k_BT$ [39,47,48].

It should be noted that the terms point of zero charge and isoelectric point are often used interchangeably, isoelectric point corresponds to the results obtained by the electrokinetic method, while the point of zero charge value is obtained by titration [32]. Plaza et al. [46] observed that for hematite particles, the pH ($\zeta = 0$) and pH ($\psi_0 = 0$) are almost identical. Alvarez-Silva et al. [49] also noted that PZC and IEP can be considered equal if no other specific adsorption of potential-determining ions happens. To avoid confusion between the surface potential of rock matrix surface and hematite particles, throughout this study we will refer to this as the point of zero charge which is where the surface charge density is zero.

2.6. Core-flood experimental setup

The core-flood experiment setup is shown in Fig. 2. The setup was placed on the couch of the CT scanner to enable monitoring of external particles migration during the core-flood experiments. A core sample was placed into a poly-ether-ether-ketone core holder, which is transparent to X-rays, and positioned in the gantry of the scanner. The core holder is oriented vertically in order to mitigate the effect of gravity on particles distribution within the injected fluid stream as well as within the core. The core holder had three differential pressure transducers (KEMA03 ATEX 1561) with ±300 mbar range and ±1 mbar accuracy to monitor pressure drop along the core during the experiment. Differential pressure was measured during core-flood experiments at the inlet, middle and outlet sections of the sample with lengths 4.1 ± 0.1 cm, 8.8 ± 0.1 cm, and 4.0 ± 0.1 cm accordingly. Pressure drop over the core was also monitored using inlet and outlet pressure transducers, while the outlet pressure was set using a backpressure regulator (BPR). Fluids were injected into the core using a Quizix pump, which was operated at a constant flow rate. A fraction collector (GE Frac 920) was used for sampling the effluents at the core-holder outlet for visual detection and physical-chemical analysis of hematite particles at the outlet.

2.7. Core-flood experimental procedure

A set of core-flood experiments was performed for this study. For the discussion in the current paper we present the results of the two most representative experiments, further referred to as Experiment 1 and Experiment 2. The same experimental procedure was applied to all tests. During Exp. 1, we investigated the effect of a gradual rise in pH from neutral up to pH 10 and during Exp. 2 a steeper rise from neutral to pH

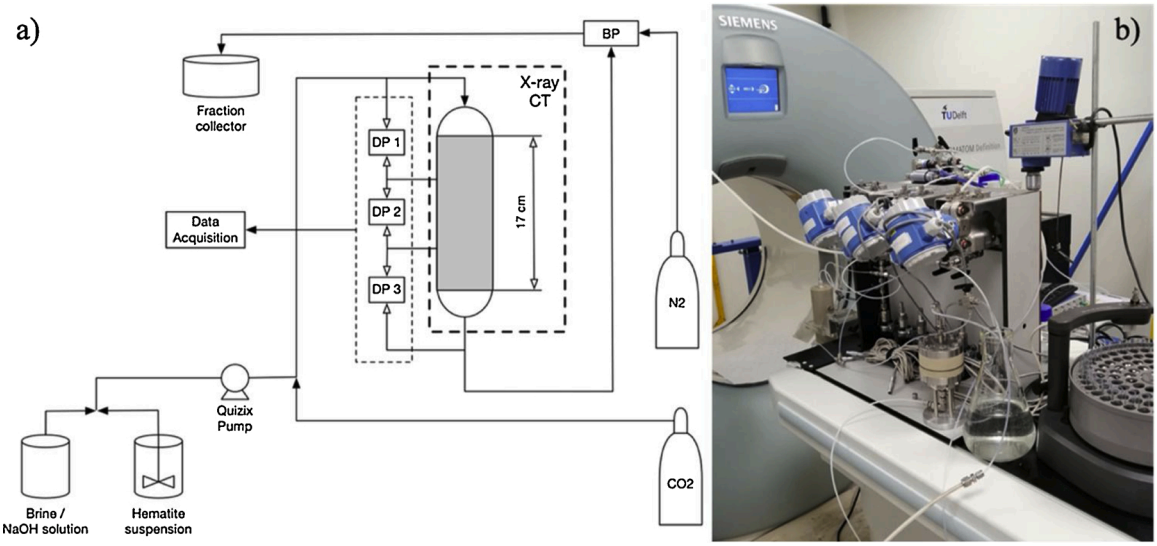

Fig. 2. a) The schematic drawing of the experimental setup used to perform the core-flood experiments. DP = differential pressure, BP = back pressure; b) photo of the setup.

12 was studied in order to investigate the effect of pH values further from PZC of hematite on the remobilization of the particles.

The tests were performed in three stages. First, the core sample was saturated with 5000 ppm NaCl brine and its permeability to brine was determined using Darcy's law [50]. Then hematite suspension in deionized water was injected at sufficiently high flow rate (25 mL/min) to prevent the gravitational segregation of the particles [35,36]. 60 pore volumes (PV) of hematite suspension were injected in Experiment 1, and 30 PV in Experiment 2. Lower volume injected in Exp. 2 was dictated by the significantly higher differential pressure observed during the experiment because of lower permeability of the core (as will be discussed in more detail in Section 3.4)

Finally, the core was subjected to the injection of deionized water at gradually increasing pH. In Exp. 1, pH steps were 7, 8, 9, 10, in the second one 7, 9, 11, and 12. The deionized water injection rate in both tests was 10 mL/min. The other experimental parameters are summarized in Table 2. Before the core-flood experiments, the deionized water was passed through 0.5 μm filter in order to prevent the effect of any solid impurities.

2.8. X-ray CT scanning

X-ray CT scanning was performed throughout the injection of both hematite suspension and deionized water in order to build hematite distribution profiles and track the movement of particles. Siemens SOMATOM Definition Dual Energy CT scanner with slice number of 64 slices per second and a resolution of 0.25 mm is used in this study. The scanning was performed at 140 KeV and 250 mA. To enable a quantitative analysis of hematite distribution along the core during core-flood experiments, we first established the calibration curve for CT scan number against hematite concentration by measuring the measured CT attenuation value (CT number) for hematite suspensions for solid phase concentrations ranging from 0 to 40,000 ppm. The resulting curve shown in Fig. 3 show that the CT attenuation varies linearly with hematite concentration.

3. Results and discussion

3.1. Sandstone characterization

The characteristics of Bentheimer sandstone were extensively discussed in the literature [34,51]. Here, we only highlight the important aspects which are relevant to our study. As can be seen in Fig. 4, the XRD analysis on the pulverized Bentheimer sample which was used for core-flood experiments shows, that it consists dominantly of quartz with very small fractions of kaolinite (99.3 ± 0.1 wt% and 0.7 ± 0.1 wt% respectively). This is in very good agreement with observations of Farooq et al. [52] and Al-Yaseri et al. [51] who found that the fraction of quartz in Bentheimer sandstone is approximately 98 and 99 wt%

Table 2
Parameters of the experiments.

	Permeability	Stage 1	Stage 2	Stage 3	Stage 4	Stage 5
Exp. 1	1770 ± 20 mD	Hematite suspension	Deionized water pH 7	pH 8	pH 9	pH 10
		Q = 25 mL/min	Q = 10 mL/min	Q = 10 mL/min	Q = 10 mL/min	Q = 10 mL/min
		V = 60 PV	V = 10 PV	V = 6 PV	V = 8 PV	V = 10 PV
Exp. 2	1400 ± 20 mD	Hematite suspension	Deionized water pH 7	pH 9	pH 11	pH 12
		Q = 25 mL/min	Q = 10 mL/min	Q = 10 mL/min	Q = 10 mL/min	Q = 10 mL/min
		V = 30 PV	V = 8 PV	V = 6 PV	V = 10 PV	V = 20 PV

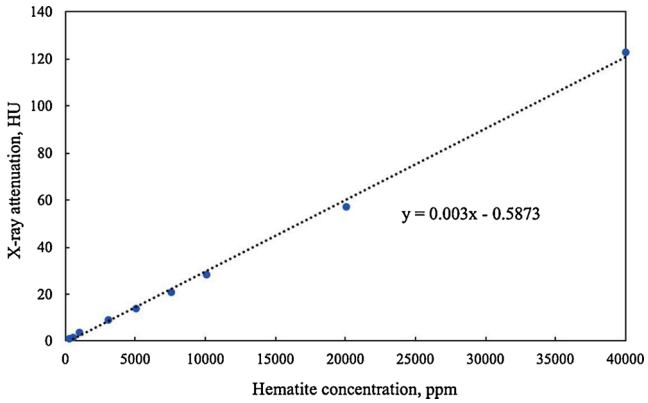

Fig. 3. Calibration curve of CT value as a function of hematite concentration. The concentration ranging from 0 to 40,000 was used. The dashed line represents the linear trend line of the concentration.

respectively with a small fraction of kaolinite (0.5 and 0.7 wt% respectively). It should be noted that in our XRD analysis, a few very small peaks were not identified. Thus, there might be some phases present, which are not included in the fraction calculation.

The dielectric behavior of the Bentheimer sample was assessed based on the alteration in surface charge as a result of the change in the pH. The surface charge of silica, as the main component of the Bentheimer sandstone, is due to adsorption or dissociation of protons on the surface and the consequent ionization of the silanol groups represented by the following reactions [53,54]:

$$SiOH + H^+ \rightarrow SiOH_2^+ \quad (10)$$

$$SiOH + OH^- \rightarrow SiO^- + H^+ \quad (11)$$

Based on the PMT method, the point of zero charge (PZC) of the Bentheimer sample was found to be 3.4 ± 0.1 (see Fig. S1 in the supplementary materials). This is in agreement with the finding of Farooq et al. [52] who also used the PMT method and whose Bentheimer sample had a quartz fraction of approximately 98 wt%. However, the value of PZC measured in this study differs from the observation of Peksa et al. [34] whose Bentheimer sample had a quartz fraction of approximately 92 wt% and measured a PZC of nearly 8. They attributed this unexpected high PZC to the presence of clay (~ 2.7 wt%) and iron particles (0.2 wt %) distributed in the sample. Further work on this matter is not within the scope of this study. Fig. 5 indicates the surface charge density and proton balance related to the dissolution effects based on the PMT data. Above the PZC, the sandstone surface was dominated by SiO^- sites and as a result, it became negatively charged. The magnitude of negative surface charge density increases with increasing pH due to the dissociation of silanol groups. Such an increase is more pronounced at pH > 7. [54] cautioned interpreting the data at pH > 7 because of possible silica dissolution. Nonetheless, it is generally accepted that with increasing pH beyond the PZC, more and more negative charges become available on the sandstone surface. The estimated values for the surface charge density in this study were in good agreement with the observation of Behrens and Grier [55] who estimated the surface charge density of a silica sample.

3.2. Colloidal stability of hematite particles

To study the colloidal stability of hematite particles, first, their zeta potential at various pH was measured in a medium with very low ionic strength ($I = 1$ mM, equivalent to 60 ppm NaCl). As shown in Fig. 6, the PZC of hematite particles was approximately 8.5 in good agreement with measurements reported by others [32,46]. At pH values above the PZC, the zeta potential values of the particles became more negative, reaching values close to −22 mV at pH 12. The measured zeta potential and PZC

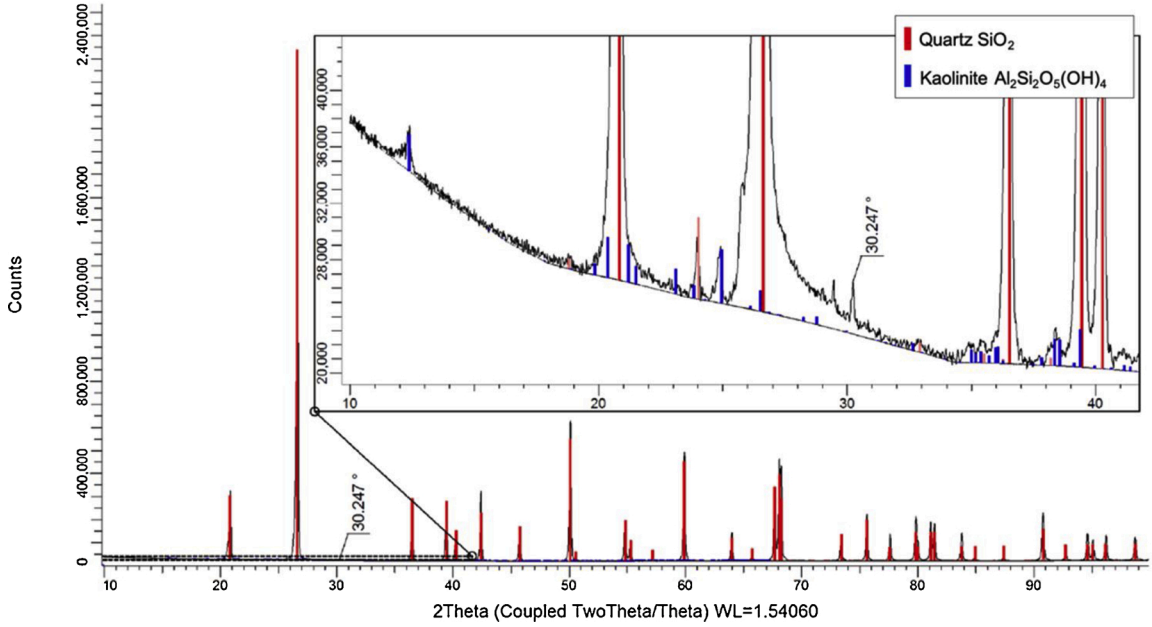

Fig. 4. XRD pattern of the pulverized Bentheimer sample used for Exp.1 1. Based on the semi-quantitative approach, silica was found to be the main compound in the rock (99.3 ± 0.1 wt%). There was also a small fraction of kaolinite (0.7 ± 0.1 wt%).

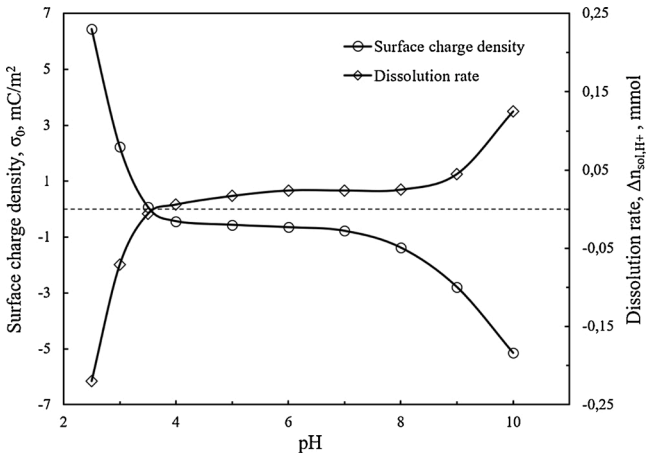

Fig. 5. Estimation of the dissolution rate and surface charge density as a function of pH for the Bentheimer sample used in the core-flood experiments based on the potentiometric mass titration data. Above the PZC = 3.4 ± 0.1, the rock surface is negatively charged.

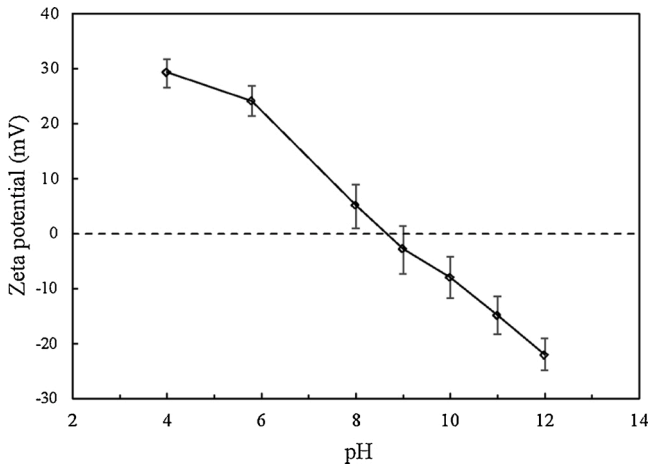

Fig. 6. Zeta potential measurements at various pH to identify the PZC of hematite particles. The PZC was found at pH 8.5 ± 0.1.

of the hematite particles agree well with values reported in the literature [36,56–58].

The relative contributions of the surface forces to particles interactions were predicted by estimating the van der Waals and electrostatic potentials using the DLVO theory (see Section 2.5). Moreover, as will be seen below, the calculations provide insights needed to choose an appropriate ionic strength and pH for the hematite suspension used in the core-floods. For this purpose, the colloidal stability of hematite particles was studied by varying (a) ionic strength and (b) pH. As shown in Eq. 4, to estimate the van der Waals potential, the Hamaker constant for hematite (A_H) must be known. The Hamaker constant for hematite particles interacting with each other across the water, as the medium, can be calculated from the Lifshitz theory, assuming small differences in dielectric and magnetic properties [59]. A Hamaker constant of 25×10^{-20} J was used for the DLVO calculations in this study [60]. The list of other parameters used in the calculations is given in Table S1 in the supplementary materials.

Fig. 7a shows the total inter-particle interaction potential as a function of particle separation distance for hematite particles at pH 5.8 by varying the ionic strength. At very low ionic strength ($I = 1$ mM), the potential barrier was approximately $110/k_BT$. This implies that colloidal stability is ensured. Nonetheless, increasing the ionic strength to 50, 85 and 200 mM led to a potential barrier smaller than $16/k_BT$ implying that the colloidal stability is not achieved. It should be noted that $I = 85$ mM is equivalent to 5000 ppm NaCl solution which is used to saturate the core prior to injection of hematite suspension.

The effect of pH on the colloidal stability of hematite particles was investigated by varying the pH from 4 to 12. As can be seen in Fig. 7b, for pH 4, 5.8, and 12 the potential barrier is larger than $16/k_BT$; however, for pH 8 and 10 the potential barrier was found to be smaller than $16/k_BT$. This is attributed to the density of charges on the surface of hematite particles. At pH close to the PZC of hematite particles, the density of charges is low and the van der Waals potential is dominant over the electrostatic potential. Nonetheless, at pH far away from PZC, as it is also evident from zeta potential measurements, the charges

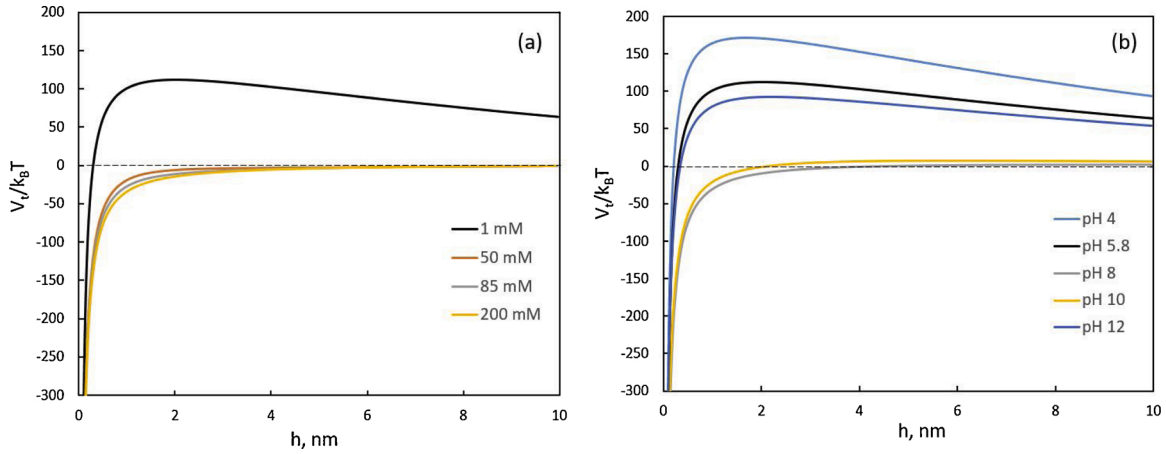

Fig. 7. Inter-particle interaction potential (V_t) as a function of particle separation distance (h) calculated by DLVO theory: a) Effect of ionic strength on hematite particle interaction at pH 5.8; b) Effect of pH on hematite particle interaction at $I = 1$ mM using zeta potential values given in Fig. 6.

density is high enough to make the electrostatic potential larger than the van der Waals potential. This ensures the colloidal stability of hematite particles. The change in colloidal stability as a function of pH is also noticeable from visual inspection and PSD measurement (see Figs. S2 and S3 in the supplementary materials which shows the suspension of hematite particles at various pH and their PSD respectively) and only the suspensions with pH far away from the PZC are colloidally stable (Tables 3 and Table 4).

3.3. Deposition of hematite particles in porous media

Based on the results of the above analysis of stability of the suspension of hematite colloidal particles, we chose to work with hematite particles dispersed in deionized water at pH 5.8 as it indicated sufficient colloidal stability. As hematite particles have a strong tendency to aggregate and form larger particles even in a very short time scale [36], the suspension was continuously stirred prior to injection to the core.

We injected suspensions with hematite concentration of 250 ppm in deionized water into the core which was saturated with 5000 ppm NaCl solution. It should be noted that with such approach pH and salinity are changed simultaneously. Although the initial contact of the suspension with brine could theoretically have provoked aggregation of hematite particles at the sample inlet, we did not detect any feasible indication of its occurrence. This can be explained by too little ion diffusion speed relative to the speed of the water front propagation. In any case, the possible particle flocculation at the initial phase of the test does not affect our further interpretation and conclusions regarding the effect of pH increase.

The estimated charge density shown in Fig. 8 reveals that in the pH ranging from 3.4 ± 0.1–8.5 ± 0.1, the hematite and rock surface have opposite charges and consequently their interaction between the particles and rock surface is dominated by electrostatic attraction whereas at pH > 8.5 ± 0.1 it is mainly by electrostatic repulsion. Therefore, by the injection of deionized water-based suspension with pH 5.8, the interaction between particles and pore walls can be expected to be dominated by an electrostatic attraction.

Table 3
Permeability of the core sample before and after Exp. 1.

	Permeability before, mD ($\mu m^2 \cdot 10^3$)	Permeability after, mD ($\mu m^2 \cdot 10^3$)	Permeability impairment
Total	1770	590	67 %
Section 1	1760	270	85 %
Section 2	1780	1010	43 %
Section 3	1760	950	46 %

Table 4
Permeability of the core sample before and after Exp. 2.

	Permeability before, mD ($\mu m^2 \cdot 10^3$)	Permeability after, mD ($\mu m^2 \cdot 10^3$)	Permeability impairment
Total	1460	240	84 %
Section 1	1470	90	94 %
Section 2	1460	500	66 %
Section 3	1450	430	70 %

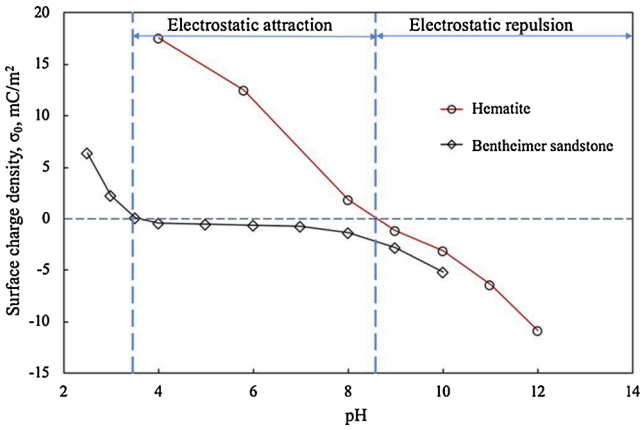

Fig. 8. The estimated surface charge density for the hematite particles and the Bentheimer sample used in the core-flood experiments. In the pH ranging from 3.4 ± 0.1 to 8.5 ± 0.1, the interaction between the particles and rock surface is dominated by the electrostatic attraction whereas at pH > 8.5 ± 0.1 is dominated by electrostatic repulsion.

Flooding with deionized water-based suspension triggered predictable in-situ clay particles detachment and migration due to salinity drop. Even though clay represented only less than 1 wt% of the dry sandstone, their presence was visually detected in the effluent as a turbidity, sampled during the first 2 PV injected (see Fig. S4 in the supplementary materials). Since the transparency of the effluent was restored upon injection of 5 PV, for the overall interpretation of the experiments we consider that such low clay content does not influence the results of the study.

In our experiments, it was observed that hematite nanoparticles affect permeability mainly in the porous medium near the inlet of the samples. Fig. 9 shows the differential pressures obtained in Exp. 1. The differential pressure in the first section rose above other sections consistently with the build-up of a filter cake due to a higher amount of particles retained and then increased almost linearly. The filter cake observed at the core inlet after the experiments is shown in Fig. 10. On the other hand, a successively smaller permeability decrease was observed in the middle and outlet section of the cores. Upon injection of 32 PV in Exp. 1 and 14 PV in the second one, hematite particles appeared in the effluent (see Fig. S4 in the supplementary material). Their concentration in the effluent consistently increased in both tests until the end of hematite suspension injection (60 PV in Experiment 1 and 30 P V in the second). Different time of filter cake build-up and particles penetration to the outlet is attributed to the difference in the core properties, permeability in particular.

The formation of the external filter cake could occur due to electrostatic retention of positively charged hematite particles by negatively charged quartz matrix. Although at later stages of deposition, when quart surfaces got considerably covered by hematite particles, they could produce lateral repulsion effects [61] screening the electrostatic attraction of quartz surfaces. At this stage size-exclusion interception of hematite micro-aggregates, formed in the suspension, could become dominant. It is believed that size-exclusion occurs if infiltrated fines size exceeds 1/6 of the mean pore diameter [62]. The contact of deionized water-based suspension with NaCl brine during its initial displacement could contribute to the aggregation of hematite particles at the core inlet. However, ion diffusion speed was theoretically predicted to be several orders of magnitude lower than the speed of concentration front propagation into the core and in our opinion this effect has negligible influence on the results of our study.

Analysis of CT-derived hematite concentration along the core during the suspension injection confirmed gradual propagation of the particles through the core, although their maximum concentration occurred within the external filter cake at the inlet surface of the cores (Fig. 11). At the horizontal axis of the graph, zero coordinate corresponds to the inlet surface of the sample, negative coordinates correspond to the accumulating external filter cake, and positive coordinates correspond to measurements within the core. The CT-derived particles distribution along the samples was in agreement with high-resolution images of the sample slab along its length, made upon completing the flooding tests (Fig. 12). Saturation of the reddish color, the characteristic of hematite particles, was maximum at the inlet side (left) of the cores and gradually decreased towards their outlet sides (right).

3.4. Mobilization of hematite fine particles by pH increase

Upon completing the injection of the hematite suspension, the core was subjected to flooding with deionized water of increasingly higher pH to initiate hematite particles transport inside the porous medium. The change in differential pressure upon switching from suspension to deionized water observed in Fig. 9 was caused by the reduction of the flow rate from 25 mL/min to 10 mL/min. In Exp. 1, the flooding with water with the pH increasing from 7 to 9 caused a gradual rise of differential pressure and consequent decrease of permeability within the inlet sections. In Exp. 2, the rise of differential pressure at same pH levels was noticeably higher. Slight differential pressure rise was also observed within the middle and outlet sections during Exp. 2. The build-up of the differential pressure in the inlet sections is believed to be mainly caused by compaction of the filter cake under the hydrodynamic pressure as well as possible partial flushing particles into the rock and increased clogging of pore throats within the core inlet section. The more pronounced pressure raise in the middle and outlet sections of the second core can be attributed to either penetration of hematite particles or migration of in-situ clays that may disperse from sand grains due to treatment with low concentrated NaOH, that was used for adjusting the pH of the fluids [71].

The increase of the injected water pH from 9 to 10 in Experiment 1 resulted in differential pressure decline within the inlet section. The differential pressure continuously decreased during the injection of the first 5 PV and stabilized upon the injection of 6 PV (Fig. 9). Differential

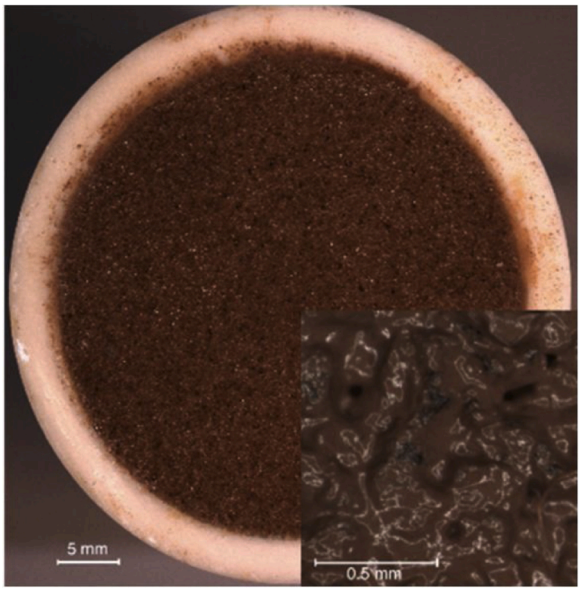

Fig. 10. Filter cake observed at the core inlet as a result of injection of hematite suspension (Exp. 1).

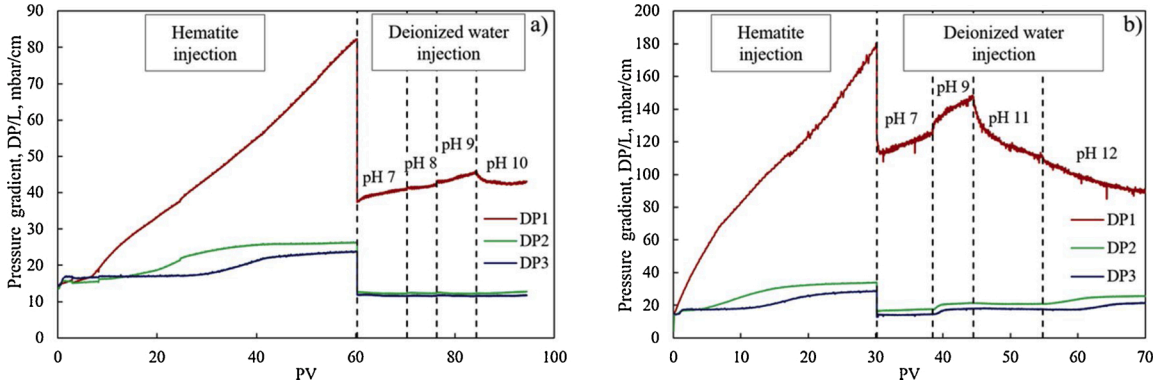

Fig. 9. Pressure gradient as the function of PV injected during core-flood experiments in three sections of the core: a) Exp. 1, injection of hematite suspension and deionized water with pH 7-10, b) Exp. 2 injection of hematite suspension and deionized water with pH 7-12.

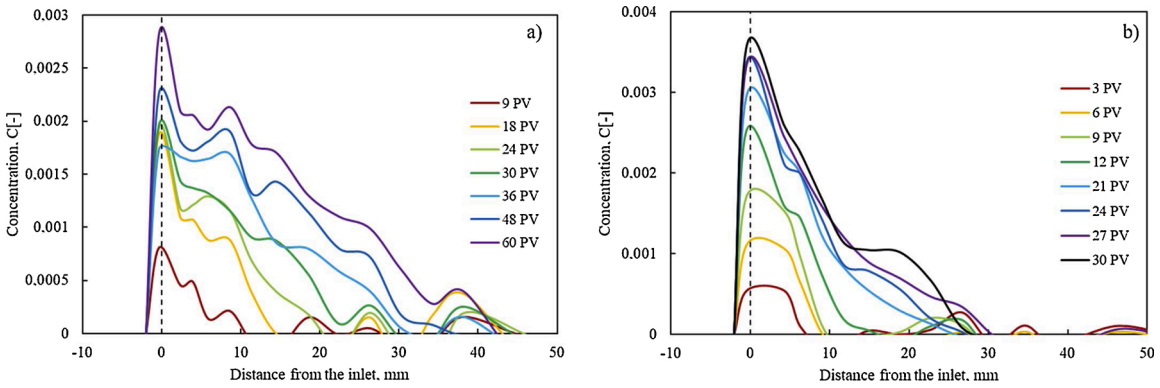

Fig. 11. Hematite concentration as a function of distance from core inlet: a) Exp. 1, from 9 PV to 60 PV, b) Exp. 2, from 3 PV to 30 PV. All the data shown correspond to section 1 of the cores.

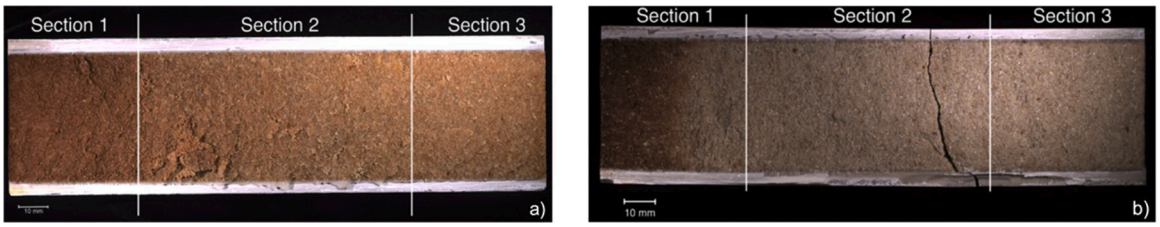

Fig. 12. Microscopic image of the core after core-flood experiments: a) Exp. 1, b) Exp. 2.

pressure in the middle and outlet section of the core, on the other hand, started slightly rising after 5 PV injected. However, in both tests no hematite presence was detected in the effluent, meaning that all released particles were still retained within the core even after the injection of a large number of PVs.

Further increase in the pH of the injected deionized water from 9 to 11 in Exp. 2 resulted in a steep decrease in the differential pressure drop in the inlet section of the core (Fig. 9). Pressure in the middle and outlet sections remained unchanged. Further increase of pH from 11 to 12 resulted in a consistent decline of the differential pressure in the inlet section and a much less pronounced rise of differential pressure in the middle and outlet sections of the core. The differential pressure decline in the inlet section persisted even upon injection of 10 PV while rising asymptotically to a final value in the middle and outlet sections. The observed pressure response to the pH increase in the middle and outlet sections in both tests was much less than in the inlet section, because the most injected colloidal particles were retained at the core inlet surface or within the first section.

The concentration of particles inside the core was monitored at different stages of both tests with CT-scan. Analysis of the CT-data showed that up to the PZC of hematite particles, the signal from the filter cake was increasing (see Fig. S5 in supplementary materials). This is in agreement with differential pressure data that indicated consolidation of the filter cake under the hydrodynamic force. After pH increased above the PZC CT-derived concentration profiles confirmed the decrease of particle concentration in the inlet core section. It should be mentioned that care must be taken to minimize unavoidable artifacts associated with CT scanning to perform reliable quantitative analysis.

4. General discussion

The purpose of this work was to study the effect of pH alteration on entrapment and remobilization of hematite colloidal particles in porous media. We investigated the charge reversal of the particles above their point of zero charge as a technique to remobilize the deposited particles and transport them in porous media.

The retention of particles and their further transport was primarily observed by the differential pressure measurements at different lengths of the core. During the hematite deposition stage, the pressure data suggested subsequent deposition of the particles in all sections of the core and formation of a filter cake in the inlet section. Injection of deionized water with pH lower than the point of zero charge of hematite particles (i.e. pH 8.5 ± 0.1) did not trigger any particles migration as the electrostatic interaction between positively charged hematite particles and negatively charged quartz grains of the rock matrix surface was attractive. Injection of deionized water at pH 9, which is slightly above the point of zero charge of hematite particles, also did not cause particles mobilization suggesting that the density of negative charges on the particles surface was not high enough to ensure an adequate electrostatic repulsion between particles and rock matrix surface that cause detachment of particles (see Fig. 8 for surface charge density of hematite particles and rock matrix at various pH). Increasing pH to 10, however, led to a decrease of differential pressure in the inlet section and its build-up downstream, indicating the start of the migration of the particles from the inlet surface further inside the core. Further increase in pH, according to the surface charge measurements, led to giving rise to a larger electrostatic repulsion term due to the increase of surface charge density of both hematite and quartz particles. The increase in surface charge density could also contribute to the deflocculation of hematite aggregates formed at the core inlet and penetration of the dispersed particles into the rock. However, the permeability restoration occurred only partially which suggests that the size-exclusion retention of the coagulated hematite particles remained, while the electrostatic retention was eliminated. Analysis of the CT-derived concentration profiles of the hematite also showed the migration of the particles associated with increasing pH.

The observed results prove the premise that above the point of zero charge, hematite particles came into repulsive interaction with the rock matrix surface which resulted in their detachment and further penetration into the core. However, we found that apart from the sign, the density of charges also plays an important role and at pH values higher but close to the point of zero charge, the density of negative charges on the surface of particles was too small to cause their remobilization.

The discussed hypothesis was previously reviewed in several studies.

In the work of Vaidya and Fogler [22] migration of in-situ kaolinite particles was observed as a function of pH and severe permeability impairment was observed after the charge reversal of the particles due to particles mobilization. A more recent work of Mahmoudi et al. [63] also observed kaolinite migration in the sandstone at high pH values. In both these studies change of salinity and pH conditions were performed and observed simultaneously whereas in our study we analyzed the influence of pH only. Generally, our work is in agreement with the aforementioned studies on the hypothesis of mobilization of particles with a pH-dependent surface charge at a high pH level. As the step forward in the ongoing research we provide a detailed theoretical study of colloidal stability of hematite particles and report the effect of surface charge density of particles and rock matrix on the electrostatic interaction between them. Moreover, we experimentally established the theoretical possibility of external particles remobilization and migration because of their charge reversal caused by pH increase, be means of variety of methods, including CT scanning technique that proved to be an effective tool for monitoring the migration of colloidal particles in the porous media throughout the experiment.

The following limitations of this work must be acknowledged. The strong tendency of hematite colloidal particles to aggregate needs to be taken into account in all stages of the particles characterization and core-flood experiments. For instance, particles tend to sediment shortly after preparation, therefore the analysis of their particle size distribution, determined by dynamic light scattering, should be done with caution. Besides, limitations of CT scanning include minimization of experimental artifacts for the quantitative analysis. These artifacts can appear on CT images as an effect of the core position inside the scanner and selected scanning parameters and they need to be minimized at the preparation stage and during image analysis. Also, the interpretation of the core-flood experiments in our study was primarily focused on the interactions between particles and rock surface. Further theoretical studies which include both rock-particle and particle-particle interactions are recommended.

As mentioned before, hematite particles were chosen for the study specifically because they have pH-dependent surface charge and are traceable under CT scan. However, we believe that the conclusions of this study can be extrapolated to real field-case applications of natural clastic reservoirs. The main mineral of such reservoirs is quartz, similar to the rock in our studies. Since the point of zero charge of quartz is lower than the naturally occurring pH, the sand grains surfaces are usually negatively charged in clastic reservoirs. Clay minerals, usually presented in the natural rocks, have very different and complex mineralogy and crystal structure, therefore their PZC can vary significantly. At the same time clay minerals, similar to colloidal particles of hematite used in this study, are hydrated in water and therefore respond to the changes in the surrounding environment. At naturally occurring pH clay particles are electrostatically attracted to quartz grains and an increase in pH can reverse their surface charge and initiate migration, as it was shown in the works mentioned above [22,63]. Therefore, we suggest that the mechanism of particle charge reversal due to an increase of pH over the PZC can result in the same behavior for clay minerals in the natural clastic rocks and other minerals with pH-dependent surface charge. This suggestion is a foundation for further detailed and comparative research.

5. Conclusions

In this work, the impact of pH alteration on entrapment and remobilization of hematite particles in a sandstone porous medium was investigated. The experiments showed that the rock surface was negatively charged at pH values higher than ~3.4 while the surface of hematite particles became negatively charged only at pH values higher than ~8.5. Injection of the hematite suspension at original pH 5.8 into the sandstone core led to the formation of a filter cake in the inlet due to the combined effect of electrostatic retention of positively charged hematite particles on negatively rock surface and size-exclusion interception of hematite micro-aggregates formed in the suspension. During the injection of deionized water with pH values up to 9, no indication of hematite particles mobilization in the filter cake was observed. At pH values higher than 9, however, a decrease of differential pressure in the inlet section was noticed, indicating the start of the migration of the particles from the inlet surface further inside the core and partial destruction of the filter cake. This was due to a change of surface charge of hematite particles from positive to negative giving rise to a repulsion term when they interact with negatively charged rock surface which ceases electrostatic retention of hematite particles and enables their further penetration into the rock porous network. Analysis of the CT-derived concentration profiles also showed the decrease of particle concentration in the inlet core section at pH values higher than 9. The results of this study provide insights into fine-tuning the electrostatic interactions in porous media and thus mitigating the permeability reduction as a result of fines migration for particles with pH-dependent surface charge.

CRediT authorship contribution statement

Anna K. Kottsova: Conceptualization, Methodology, Validation, Formal analysis, Investigation, Resources, Writing - original draft, Writing - review & editing. **Mohsen Mirzaie Yegane:** Supervision, Methodology, Investigation, Resources, Writing - review & editing. **Alexei A. Tchistiakov:** Conceptualization, Methodology, Validation, Writing - review & editing, Supervision. **Pacelli L.J. Zitha:** Conceptualization, Methodology, Validation, Resources, Writing - review & editing, Supervision.

Declaration of Competing Interest

The authors report no declarations of interest.

Acknowledgements

This work was supported by the Ministry of Science and Higher Education of the Russian Federation under agreement No. 075-15-2020-119 within the framework of the development program for a world-class Research Center. We thank the Ministry of Science and Higher Education of the Russian Federation for its support.

The authors gratefully acknowledge the Skolkovo Institute of Science and Technology (Russia) and Delft University of Technology (The Netherlands) for providing their laboratories facilities for the experiments. The authors thank Michiel Slob, Jolanda van Haagen, Marc Friebel, and Ellen Meijvogel-de Koening for technical support. The authors also acknowledge Martijn Janssen, Swej Shah, and Sian Jones for fruitful discussions.

Appendix A. Supplementary data

Supplementary data associated with this article can be found, in the online version, at https://doi.org/10.1016/j.colsurfa.2021.126371.

References

[1] L.M. McDowell-Boyer, J.R. Hunt, N. Sitar, Particle transport through porous media, Water Resour. Res. 22 (13) (1986) 1901–1921, https://doi.org/10.1029/WR022i013p01901.
[2] S. Torkzaban, S.A. Bradford, S.L. Walker, Resolving the coupled effects of hydrodynamics and DLVO forces on colloid attachment in porous media, Langmuir 23 (19) (2007) 9652–9660, https://doi.org/10.1021/la700995e.
[3] E. Rosenbrand, C. Kjøller, J.F. Riis, F. Kets, I.L. Fabricius, Different effects of temperature and salinity on permeability reduction by fines migration in Berea sandstone, Geothermics 53 (2015) 225–235, https://doi.org/10.1016/j.geothermics.2014.06.004.
[4] J.W. Jung, J. Jang, J.C. Santamarina, C. Tsouris, T.J. Phelps, C.J. Rawn, Gas production from hydrate-bearing sediments: the role of fine particles, Energy Fuels 26 (1) (2012) 480–487, https://doi.org/10.1021/ef101651b.

[5] M. Byrne, I. Patey, J. Green, A New Tool for Exploration and Appraisal-Formation Damage Evaluation, 2007.

[6] M.J. Alshakhs, A.R. Kovscek, Understanding the role of brine ionic composition on oil recovery by assessment of wettability from colloidal forces, Adv. Colloid Interface Sci. 233 (2016) 126–138, https://doi.org/10.1016/j.cis.2015.08.004.

[7] S. Iglauer, S. Favretto, G. Spinelli, G. Schena, M.J. Blunt, X-ray tomography measurements of power-law cluster size distributions for the nonwetting phase in sandstones, Phys. Rev. E Stat. Nonlin. Soft Matter Phys. 82 (5 Pt 2) (2010), 056315, https://doi.org/10.1103/PhysRevE.82.056315.

[8] R.A. Nasralla, M.A. Bataweel, H.A. Nasr-El-Din, Investigation of wettability alteration and oil-recovery improvement by low-salinity water in Sandstone Rock, J. Can. Pet. Technol. 52 (02) (2013) 144–154, https://doi.org/10.2118/146322-PA.

[9] E. Pooryousefy, Q. Xie, Y. Chen, A. Sari, A. Saeedi, Drivers of low salinity effect in sandstone reservoirs, J. Mol. Liq. 250 (2018) 396–403, https://doi.org/10.1016/j.molliq.2017.11.170.

[10] H. Lei, L. Dong, C. Ruan, L. Ren, Study of migration and deposition of micro particles in porous media by Lattice-Boltzmann Method, Energy Procedia 142 (2017) 4004–4009, https://doi.org/10.1016/j.egypro.2017.12.317.

[11] R.N. Vaidya, H.S. Fogler, Formation damage due to colloidally induced fines migration, Colloids Surf. 50 (1990) 215–229, https://doi.org/10.1016/0166-6622(90)80265-6.

[12] M. Elimelech, Kinetics of capture of colloidal particles in packed beds under attractive double layer interactions, J. Colloid Interface Sci. 146 (1991) 337–352.

[13] M. Elimelech, J. Gregory, X. Xia, R.A. Williams, Particle Deposition and Aggregation, paperback ed, Butterworth-Heinemann, Oxford, 1995.

[14] A.A. Tchistiakov, Colloid chemistry of in-situ clay-induced formation damage, SPE International Symposium on Formation Damage Control, Lafayette (2000) 371–379, https://doi.org/10.2523/58747-ms.

[15] A. Tchistiakov, Physico-chemical aspects of clay migration and injectivity decrease of geothermal clastic reservoirs, Proceedings World Geothermal Congress (2000) 3087–3095.

[16] A. Tchistiakov, Physico-chemical factors controlling in-situ clay-induced formation damage during water re-injection, in: Proceedings of ETCE 2000 & OMAE 2000 Joint Conference Energy for the New Millennium, New Orleans, USA, 2000, pp. 14–17. February.

[17] A. Kalantariasl, P. Bedrikovetsky, Stabilization of external filter cake by colloidal forces in a "Well–Reservoir" system, Ind. Eng. Chem. Res. 53 (2) (2014) 930–944, https://doi.org/10.1021/ie402812y.

[18] S.F. Kia, H.S. Fogler, M.G. Reed, Effect of pH on colloidally induced fines migration, J. Colloid Interface Sci. 118 (1) (1987) 158–168, https://doi.org/10.1016/0021-9797(87)90444-9.

[19] S.F. Kia, H.S. Fogler, M.G. Reed, R.N. Vaidya, Effect of salt composition on clay release in Berea sandstones, Spe Prod. Eng. 2 (04) (1987) 277–283, https://doi.org/10.2118/15318-PA.

[20] A. Al-Sarihi, A. Zeinijahromi, L. Genolet, A. Behr, P. Kowollik, P. Bedrikovetsky, Effects of Fines Migration on Residual Oil during Low-Salinity Waterflooding, Energy Fuels 32 (8) (2018) 8296–8309, https://doi.org/10.1021/acs.energyfuels.8b01732.

[21] S. Borazjani, D. Kulikowski, K. Amrouch, P. Bedrikovetsky, Composition changes of hydrocarbons during secondary petroleum migration, APPEA J. 58 (2018) 784, https://doi.org/10.1071/AJ17127.

[22] R.N. Vaidya, H.S. Fogler, Fines migration and formation damage: influence of pH and ion exchange, Society of Petroleum Engineers - SPE Production Engineering 1992 (1992) 325–330. November.

[23] F. Mietta, C. Chassagne, J.C. Winterwerp, Shear-induced flocculation of a suspension of kaolinite as function of pH and salt concentration, J. Colloid Interface Sci. 336 (1) (2009) 134–141, https://doi.org/10.1016/j.jcis.2009.03.044.

[24] M. Kobayashi, H. Nanaumi, Y. Muto, Initial deposition rate of latex particles in the packed bed of zirconia beads, Colloids Surf. A: Physicochem. Eng. Aspects 347 (2009) 2–7.

[25] Z. You, K. Aji, A. Badalyan, P. Bedrikovetsky, Effect of nanoparticle transport and retention in oilfield rocks on the efficiency of different nanotechnologies in oil industry, Society of Petroleum Engineers - SPE International Oilfield Nanotechnology Conference 2012 (2012) 397–411, https://doi.org/10.2118/157097-ms. June.

[26] N. Kumar, M.P. Andersson, D. van den Ende, F. Mugele, I. Siretanu, Probing the surface charge on the basal Planes of kaolinite particles with high-resolution atomic force microscopy, Langmuir 33 (50) (2017) 14226–14237, https://doi.org/10.1021/acs.langmuir.7b03153.

[27] H. van Olphen, An Introduction to Clay Colloid Chemistry, Interscience Publications (New York), 1963.

[28] V.I. Osipov, Nature of Strength and Deformation Properties of Clay Rocks, Moscow, in Russian, 1979.

[29] J.K. Mitchell, Fundamentals of Soil Behavior, John Wiley & Sons, Inc, 1993.

[30] P.L. Churcher, P.R. French, J.C. Shaw, L.L. Schramm, Rock Properties of Berea Sandstone, Baker Dolomite, and Indiana Limestone, SPE International Symposium on Oilfield Chemistry, Anaheim, California, 1991, pp. 431–446, https://doi.org/10.2118/21044-MS. January.

[31] M. Didier, A. Chaumont, T. Joubert, I. Bondino, G. Hamon, Contradictory trends for smart water injection method: role of pH and salinity from sand/oil/brine adhesion maps, Int. Symp. Soc. Core Analysts 12 (2015).

[32] M. Kosmulski, Isoelectric points and points of zero charge of metal (hydr)oxides : 50 years after Parks' review, Adv. Colloid Interface Sci. 238 (2016) 1–61, https://doi.org/10.1016/j.cis.2016.10.005.

[33] B.K. Schroth, G. Sposito, Surface charge properties of kaolinite, Clays Clay Miner. 45 (1) (1997) 85–91.

[34] A.E. Peksa, K.H.A.A. Wolf, E.C. Slob, Ł. Chmura, P.L.J. Zitha, Original and pyrometamorphical altered Bentheimer sandstone; petrophysical properties, surface and dielectric behavior, J. Pet. Sci. Eng. 149 (2017) 270–280, https://doi.org/10.1016/j.petrol.2016.10.024.

[35] D. Dickson, G. Liu, C. Li, G. Tachiev, Y. Cai, Dispersion and stability of bare hematite nanoparticles: effect of dispersion tools, nanoparticle concentration, humic acid and ionic strength, Sci. Total Environ. 419 (2012) 170–177, https://doi.org/10.1016/j.scitotenv.2012.01.012.

[36] Y.T. He, A.J. Wan, At. Tokunaga, Kinetic stability of hematite nanoparticles : the effect of particle sizes, J. Nanoparticle Res. 10 (2008) 321–332, https://doi.org/10.1007/s11051-007-9255-1.

[37] J. Lützenkirchen, T. Preocanin, D. Kovačević, V. Tomišić, L. Lövgren, N. Kallay, Potentiometric titrations as a tool for surface charge determination, Croat. Chem. Acta 85 (2012) 391–417.

[38] E.M. Hotze, T. Phenrat, G.V. Lowry, Nanoparticle aggregation: challenges to understanding transport and reactivity in the environment, J. Environ. Qual. 39 (6) (2010) 1909–1924.

[39] M. Mirzaie Yegane, F.S. Minaye Hashemi, F. Vercauteren, N. Meulendijks, R. Gharbi, P.E. Boukany, P.L.J. Zitha, Rheological response of a modified polyacrylamide – silica nanoparticles hybrid at high salinity and temperature, Soft Matter 16 (2020) 10198–10210, https://doi.org/10.1039/d0sm01254h.

[40] S. Skoglund, T.A. Lowe, J. Hedberg, E. Blomberg, I.O. Wallinder, S. Wold, M. Lundin, Effect of laundry surfactants on surface charge and colloidal stability of silver nanoparticles, Langmuir 29 (28) (2013) 8882–8891.

[41] J. Israelachvili, Intermolecular and Surface Forces, 3rd edition, Academic Press, 2011.

[42] S.R. Raghavan, J. Hou, G.L. Baker, S.A. Khan, Colloidal interactions between particles with tethered nonpolar chains dispersed in polar media: direct correlation between dynamic rheology and interaction parameters, Langmuir 16 (3) (2000) 1066–1077.

[43] H. Ohshima, Effective surface potential and double-layer interaction of nanoparticles, J. Colloid Interface Sci. 174 (1) (1995) 45–52.

[44] T.F. Tadros, General Principles of Colloid Stability and the Role of Surface Forces, Wiley-VCH Verlag GmbH & Co. KGaA, 2014, pp. 1–22.

[45] L.A. Wijenayaka, M.R. Ivanov, C.M. Cheatum, A.J. Haes, Improved parametrization for extended Derjaguin, Landau, Verwey, and Overbeek predictions of functionalized gold nanosphere stability, J. Phys. Chem. C 119 (18) (2015) 10064–10075.

[46] R.C. Plaza, F. González-Caballero, A.V. Delgado, Electrical surface charge and potential of hematite/yttrium oxide core–shell nanoparticles, Colloid Polym. Sci. 279 (12) (2001) 1206–1211, https://doi.org/10.1007/s003960100578.

[47] J.C. Berg, An Introduction to Interfaces & Colloids the Bridge to Nanoscience, World Scientific Publishing Co. Pte. Ltd, Singapore, 2010.

[48] M. Moskovits, B. Vlčková, Adsorbate-induced silver nanoparticle aggregation kinetics, J. Phys. Chem. B 109 (31) (2005) 14755–14758.

[49] M. Alvarez-Silva, M. Mirnezami, A. Uribe-Salas, J.A. Finch, Point of zero charge, isoelectric point and aggregation of phyllosilicate minerals, Can. Metall. Q. 49 (2010) 405–410, https://doi.org/10.1179/cmq.2010.49.4.405.

[50] H. Darcy, Les Fontaines Publiques de la Ville de Dijon, Dalmont, Paris, 1856.

[51] A.Z. Al-Yaseri, M. Lebedev, S.J. Vogt, M.L. Johns, A. Barifcani, S. Iglauer, Pore-scale analysis of formation damage in Bentheimer sandstone with in-situ NMR and micro-computed tomography experiments, J. Pet. Sci. Eng. 129 (2015) 48–57.

[52] U. Farooq, M.T. Tweheyo, J. Sjöblom, G. Øye, Surface characterization of model, outcrop, and reservoir samples in low salinity aqueous solutions, J. Dispers. Sci. Technol. 32 (4) (2011) 519–531.

[53] J.A. Davis, R.O. James, J.O. Leckie, Surface ionization and complexation at the oxide/water interface: I. Computation of electrical double layer properties in simple electrolytes, J. Colloid Interface Sci. 63 (3) (1978) 480–499.

[54] J. Lecourtier, L.T. Lee, G. Chauveteau, Adsorption of polyacrylamides on siliceous minerals, Colloids Surf. 47 (1990) 219–231.

[55] S.H. Behrens, D.G. Grier, The charge of glass and silica surfaces, J. Chem. Phys. 115 (14) (2001) 6716–6721.

[56] M. Kosmulski, The pH-dependent surface charging and the points of zero charge, J. Colloid Interface Sci. 253 (1) (2002) 77–87.

[57] M. Kosmulski, pH-dependent surface charging and points of zero charge III. Update, J. Colloid Interface Sci. 298 (2) (2006) 730–741.

[58] C.-y. Xu, K.-y. Deng, J.-y. Li, R.-k. Xu, Impact of environmental conditions on aggregation kinetics of hematite and goethite nanoparticles, J. Nanoparticle Res. 17 (10) (2015) 394.

[59] B. Faure, G. Salazar-Alvarez, L. Bergström, Hamaker constants of iron oxide nanoparticles, Langmuir 27 (14) (2011) 8659–8664.

[60] E. Rohem Peçanha, M.D. da Fonseca de Albuquerque, R. Antoun Simão, L. de Salles Leal. Filho, M.B. de Mello Monte, Interaction forces between colloidal starch and quartz and hematite particles in mineral flotation, Colloids Surf. A Physicochem. Eng. Asp. 562 (2019) 79–85.

[61] M. Kobayashi, M. Ookawa, S. Yamada, The effects of surface charging properties on colloid transport in porous media, Appl. Mech. J. 17 (2014) 743–752.

[62] F. Civan, Reservoir Formation Damage, 3rd edition, Elsevier Inc, 2016, https://doi.org/10.1016/B978-0-12-801898-9.00028-X.

[63] M. Mahmoudi, V. Fattahpour, A. Nouri, M. Leitch, An experimental investigation of the effect of pH and salinity on Sand control performance for heavy oil thermal production, in: SPE Canada Heavy Il Technical Conference, Calgary, 2016, p. 18, https://doi.org/10.2118/180756-MS. June.

[71] V.I. Osipov, V.N. Sokolov, N.A. Rumiantseva, Microstructure of Clay Rocks, Moscow, Nedra. In Russian, 1989.
[72] S. Priisholm, B.L. Nielson, O. Haslund, Fines migration, blocking, and clay swelling of potential geothermal sandstone reservoirs, Denmark, SPE Form. Eval. (1987) 168–178, https://doi.org/10.2118/15199-PA.
[73] A. Rostami, H. Nasr-El-Din, A new technology for filter cake removal, in: Society of Petroleum Engineers - SPE Russian Oil and Gas Technical Conference and Exhibition 2010, RO and G 10, 2, 2010, pp. 1063–1079. October.
[74] T. Russell, L. Chequer, A. Badalyan, A. Behr, L. Genolet, P. Kowollik, P. Bedrikovetsky, Systematic laboratory and modelling study of kaolinite in rocks on formation-damage-fines-migration non-equilibrium effects, analytical model, Proceedings - SPE International Symposium on Formation Damage Control, 2018-Febru (2018), https://doi.org/10.2118/189533-ms.
[75] T. Russell, L. Chequer, S. Borazjani, Z. You, A. Zeinijahromi, P. Bedrikovetsky, Formation Damage by Fines Migration : Mathematical and Laboratory Modeling, Field Cases, Elsevier, Amsterdam, 2018, pp. 69–175, https://doi.org/10.1016/B978-0-12-813782-6.00003-8.
[76] A.K. Sarkar, M.M. Sharma, Fines migration in two-phase flow, J. Pet. Technol. (1990) 646–652. May.
[77] M.M. Sharma, Y.C. Yortsos, Fines migration in porous media, AIChE J. 10 (33) (1987) 1654–1662.
[78] J. Sheng, Modern Chemical Enhanced Oil Recovery: Theory and Practice, Gulf: Burlington, MA, USA, 2010.
[79] A.A. Tchistiakov, V.N. Sokolov, V.I. Osipov, Saponite clay tailing treatment by artificial sedimentation, in: Adachi, Fukue (Eds.), Clay Science for Engineering, Balkema, Rotterdam, 2001. ISBN 9058091759.